Journal of Structural Biology 191 (2015) 263–271

Contents lists available at ScienceDirect

Journal of Structural Biology

journal homepage: www.elsevier.com/locate/yjsbi

Austromegabalanus psittacus barnacle shell structure and proteoglycan localization and functionality

M.S. Fernández *, J.I. Arias, A. Neira-Carrillo, J.L. Arias

Faculty of Veterinary Sciences, University of Chile, Santiago, Chile

ARTICLE INFO

Article history:
Received 11 March 2015
Received in revised form 10 August 2015
Accepted 11 August 2015
Available online 11 August 2015

Keywords:
Barnacle
Biomineralization
Chitin
Proteoglycans
Shell

ABSTRACT

Comparative analyzes of biomineralization models have being crucial for the understanding of the functional properties of biominerals and the elucidation of the processes through which biomacromolecules control the synthesis and structural organization of inorganic mineral-based biomaterials. Among calcium carbonate-containing bioceramics, egg, mollusk and echinoderm shells, and crustacean carapaces, have being fairly well characterized. However, Thoraceca barnacles, although being crustacea, showing molting cycle, build a quite stable and heavily mineralized shell that completely surround the animal, which is for life firmly cemented to the substratum. This makes barnacles an interesting model for studying processes of biomineralization. Here we studied the main microstructural and ultrastructural features of *Austromegabalanus psittacus* barnacle shell, characterize the occurrence of specific proteoglycans (keratan-, dermatan- and chondroitin-6-sulfate proteoglycans) in different soluble and insoluble organic fractions extracted from the shell, and tested them for their ability to crystallize calcium carbonate in vitro. Our results indicate that, in the barnacle model, proteoglycans are good candidates for the modification of the calcite crystal morphology, although the cooperative effect of some additional proteins in the shell could not be excluded.

1. Introduction

The formation of mineralized structures, such as bones, teeth, shells, carapaces, corals and pearls, is a widespread phenomenon among living organisms (Lowenstam and Weiner, 1989; Mann et al., 1989; Simkiss and Wilbur, 1989). Comparative analyzes of these biomineralization models have being crucial for the understanding of the functional properties of biominerals and the elucidation of the processes through which biomacromolecules control the synthesis and structural organization of inorganic mineral-based biomaterials. Although these natural composite bioceramics contain single inorganic phases, mainly calcium carbonate or phosphate, they have unique morphologies and properties, and are assembled in aqueous solution, at ambient conditions, and to net shape (Heuer et al., 1992). The controlling activity of a relatively small repertoire and minute quantities of organic macromolecules which regulate the formation of these structures (Albeck et al., 1996; Arias et al., 1993; Belcher et al., 1996, 2000; Falini et al., 1996; Fernandez et al., 2001; Orme et al., 2001), and the hierarchical structural organization of their organic and inorganic phases play crucial roles in the mechanical properties of these natural materials (Kamat et al., 2000; Smith et al., 1999; Su et al., 2002). Some of the macromolecules involved in biomineralization of different structures are well characterized, although their role on the regulation of crystal nucleation, growth and morphology is not well understood (Dauphin, 2001; Nys et al., 1999). There has been growing interest in the principles governing the composition, structure, organization and methods of assembly of a variety of biological ceramics. Part of this interest stems from the desire to create new synthetic materials inspired by the processes involved in the formation of such bioceramics. Among calcium carbonate-containing bioceramics, egg, mollusk and echinoderm shells, and crustacean carapaces, have being fairly well characterized. While eggshell is built inside an assembly line tube during a short period of time (Arias et al., 1993; Fernandez et al., 1997, 2001), mollusk shell grows continuously without any spatial restriction (Checa and Rodríguez-Navarro, 2001), and crustacea exoskeleton grows step by step between molting periods. However, the Thoraceca barnacles, although being crustacea, showing molting cycle, build a quite stable and heavily mineralized calcite shell that completely surround the animal, which is for life firmly cemented to the substratum (Kamino et al., 2000). This makes barnacles an interesting

* Corresponding author at: Fac. Ciencias Veterinarias, Universidad de Chile, Casilla 2, Correo 15, La Granja, Santiago, Chile.
E-mail address: sofernan@uchile.cl (M.S. Fernández).

http://dx.doi.org/10.1016/j.jsb.2015.08.005
1047-8477/

model for studying processes of biomineralization. Since Darwin's descriptive studies after traveling to Chile (Darwin, 1854), there have been some studies on barnacle shell formation and general structure (Bourget, 1977), but only a few have been concerned with the chemical composition and microstructure of its shell (Fernandez et al., 2002; Lowenstam et al., 1992; Rodríguez-Navarro et al., 2006). To better understand the process of shell mineralization in the Chilean barnacle shell, we have studied the shell construction and distribution of organic components in the different structural parts of its shell using a variety of biochemical, spectroscopic and microscopy techniques. To define the functionality of different macromolecules in the mineralization process, we have studied their effect on calcium carbonate crystallization.

2. Materials and methods

Twenty shells from specimens of *Austromegabalanus psittacus* barnacles collected along the coast of Chile were used for this study.

2.1. Microstructural features

Pieces of barnacle shell were washed, dried and polished with abrasive paper N° 150 in a Vorsicht FE024HF machine to obtain thin sheets of 10–50 μm thickness. Pieces were mounted on slides and examined with light and epifluorescent microscope.

2.2. Ultrastructural features

For scanning electron microscopy (SEM), pieces of shell were polished to obtain thin sheets, decalcified for 15, 30 and 50 s with 37% orthophosphoric acid, dehydrated, coated with gold and observed in a Tesla BS 343A scanning electron microscope.

For transmission electron microscopy (TEM), samples were fixed in 2% Paraformaldehyde, 0.2% Glutaraldehyde in 200 mM phosphate buffer pH 7.4 for 48 h, decalcified in 10% formic acid for 48 h at room temperature, dehydrated in a graded acetone series and embedded in Poly Bed 812 (Polysciences Inc., Warrington, PA). Ultrathin sections (70–90 nm) were cut with a Porter Bloom MT2-B ultramicrotome.

For precise proteoglycan determination by immunogold localization, sections were incubated with one of the primary monoclonal anti-glycosaminoglycan antibodies listed below and then incubated with gold conjugated second antibody (Ted Pella, CA). Observations were made with a Zeiss EM-109 electron microscope.

The monoclonal antibodies used for this study were produced and characterized by Bruce Caterson and co-workers against specific epitopes present in proteoglycan substructures located in the sulfated glycosaminoglycans, either in saturated disaccharides or in the unsaturated disaccharides that are produced after digestion with specific endoglycosidic enzymes (Caterson et al., 1987). These antibodies do not cross-react with proteins or other saccharide epitopes. The antibodies used were:

2B6 (IgG, ICN Biomedical Inc.): this mouse monoclonal antibody specifically binds to the unsaturated disaccharide produced after digestion of dermatan sulfate (DS) or chondroitin-4-sulfate (C-4-S) by chondroitinase ABC (EC 4.2.2.4) or after digestion of chondroitin-4-sulfate by chondroitinase ACII (EC 4.2.2.5) (Caterson et al., 1985, 1987; Christner et al., 1980).

3B3 (IgM, ICN Biomedical Inc.): this mouse monoclonal antibody recognizes chondroitin-6-sulfate (C-6-S) after digestion with chondroitinase ABC (EC 4.2.2.4) or chondroitinase ACII (EC 4.2.2.5) (Caterson et al., 1985).

5D4 (IgG, ICN Biomedical Inc.): this mouse monoclonal antibody recognizes a hypersulfated hexasaccharide of keratan sulfate (KS) (Mehmet et al., 1986).

2.3. In vitro crystallization features

For organic matrix extraction, Dot-blot characterization and in vitro crystallization assays, pieces of shell were decalcified by using 10% formic acid for 13 days at 4 °C or Dowex resin (Albeck et al., 1996) in a rotating glass tube for 3 days at room temperature and dialyzed (Spectra/Por membrane tubing MWCO 3,500) with distilled water. The material inside the dialyzing bags was centrifuged and the precipitate and supernatant were separately lyophilized. Product of this centrifugation, a gross insoluble (GIF) and a soluble fraction (SF) were obtained. By freezing GIF in liquid nitrogen and ground it in a mortar and pestle to a homogeneous powder, an insoluble fraction (IF) was obtained. A deproteinized insoluble fraction (DIF) was obtained by treating a subsample of IF with 1 M NaOH at 37 °C for varied times up to 24 h, washed with a pre-determined volume of distilled water and dried (No and Meyers, 1997; Percot et al., 2003). Fourier transform infrared spectroscopy (FTIR) analysis was performed on dried flake samples. FTIR spectra were obtained with an ATR/FTIR interspec 200-X spectrometer, Estonia. The spectroscopic measurements on samples were performed directly using the PIKE Miracle TM accessory in a Ge single reflection crystal plate. The FTIR spectrum performed on a flat tip was obtained by averaging 20 scans over the spectral range of 600–4000 cm^{-1}.

A subfraction of IF obtained after Dowex resin decalcification was processed to prepare a proteoglycan-enriched fraction (PGEF) (Arias et al., 1992; Carrino et al., 1994; Yanagishita and Hascall, 1984). Briefly, the IF lyophilized subsample was solubilized in a solution of 4 M guanidinium chloride, 0.05 M sodium acetate, pH 5.8. The samples were chromatographed on Sephadex G-50 (Pharmacia) columns eluted with 8 M urea, 0.15 M sodium chloride, 0.5% CHAPS, 0.05 M sodium acetate, pH 6.0, and the V0 material was loaded onto a DEAE Sephacel column that was equilibrated in the same solution. Proteoglycans are negatively charged molecules, which adsorb to DEAE-Sephacel. After the column was rinsed with loading buffer to remove the tissue proteins, the proteoglycans were eluted in a stepwise fashion with 0.25 M and then 1.0 M sodium chloride, both in 8 M urea, 0.5% CHAPS, 0.05 M sodium acetate, pH 6.0. The PEF was lyophilized.

Dot-blots of the SF and PGEF were performed with a Bio-Dot microfiltration apparatus (Bio-Rad, Richmond, CA), as previously described (Arias et al., 1992; Lennon et al., 1991). Briefly, samples in TBS were blotted onto nitrocellulose membranes (Bio-Rad) and the membranes blocked with 3% BSA in TBS-Tween (TBS with 0.05% Tween 20). The membranes were then incubated in primary antibody at 1:500 to 1:1000 dilution in 3% BSA in TBS-Tween. After three rinses in TBS-Tween, the membranes were incubated in secondary antibody, alkaline phosphatase-conjugated goat anti-mouse IgG (Promega, obtained from Fisher, Pittsburgh, PA), which was diluted 1:7500 in TBS-Tween. The secondary antibodies were the same antibodies used for immunoultrastructural localization. After three rinses in TBS-Tween, the membranes were incubated in alkaline phosphatase substrate, nitrotetrazolium blue and 5-bromo-4-chloro-3-indolyl phosphate. The color development was stopped by rinsing the membranes with distilled water and allowing them to air dry. It is safe to indicate that the intensity of the color allows semiquatitative estimation of the concentration of the same proteoglycan present in the sample treated with the same antibody. That is, the different intensity of the color in samples treated with different antibodies does not correlate with the relative concentration of the proteoglycans present.

Control samples for the various antibodies were prepared by previously described procedures. Cartilage proteoglycans from bovine nasal septum and from Day 8 chick limb bud chondrocyte cultures were isolated by CsCl density gradient centrifugation of guanidine hydrochloride extracts (Lennon et al., 1991). The former were isolated by two sequential gradients, one associative and the second dissociative (Al-Dl); the latter were isolated by a direct dissociative gradient followed by further purification by Sepharose CL-2B molecular sieve chromatography in 4 M guanidine hydrochloride. These proteoglycans were used as positive controls for antibodies to C-6-S, DS and KS. Proteoglycans from rat chondrosarcoma, isolated similar to those from bovine nasal septum (aAl-Dl), were used as the negative control for the KS antibodies, since these proteoglycans lack KS (Caterson et al., 1983). All of these proteoglycans were used at amounts based on the dry weight of lyophilized proteoglycan and were treated with CSase AC II prior to dot-blotting in order to better expose the KS and core protein epitopes. Omission of primary antibody from the dot-blots resulted in the generation of virtually no reactivity for all of the antibodies tested.

Organic matrix fractions (insoluble fraction, soluble fraction, deproteinized soluble fraction, proteoglycan enriched fraction) obtained were assayed for their crystallization modification abilities. To determine the effect of these fractions on $CaCO_3$ crystals formation, the gas diffusion method was used (Dominguez-Vera et al., 2000; Jiménez-Lopez et al., 2003). Crystallization experiments were done using a chamber consisting of 85 mm plastic Petri dish having a 10 mm central hole in its bottom glued to a plastic cylindrical vessel. Inside the chamber, polystyrene microbridges (Hampton Res, Aliso Viejo, CA) were filled with 35 µl of 200 mM calcium chloride solution in 200 mM TRIS buffer pH 9. The cylindrical vessel contained 25 mM ammonium carbonate. Control samples contained only calcium chloride solution, while to the experimental ones, 64 µg/ml of the different fractions solution in 200 mM calcium chloride solution in 200 mM TRIS buffer pH 9 was added.

All experiments were carried out inside the petri dish at 20 °C for variable periods of time (6–20 h). Precipitation of calcium carbonate results from the diffusion of carbon dioxide vapor into the buffered $CaCl_2$ solution. Under these conditions, without any additive, only calcite crystals are formed (Neira et al., 2004). Crystals were observed in a Tesla BS 343A scanning electron microscope.

3. Results

3.1. Gross anatomical nomenclature

Barnacle shell gross anatomy has been reported elsewhere (Bourget, 1977). However, for better comprehension it is briefly recapitulated here. Shell is composed of twelve calcitic plates, six parietes and six radii, forming together a truncated cone virtually opened at the top, and linked at the bottom through an interdigitated junction with the calcareous basal disk which is firmly cemented to the rock (Fig. 1). The six parietes are arranged in a rostral paries or rostrum, two lateral and two carino lateral parietes, and one carino paries or carina. The upper part of the inner side of the plates showed a calcified thickening, the sheath, to which the opercular membrane is attached. This operculum is attached to the sheath by a soft membrane, and closes the orifice separating the outside from the crustacea soft tissues. Plates are not completely solid but show porosity due to the occurrence of longitudinal tubes or canals in the parietes (from the base to the apex) and transversal ones, running parallel to the base, in the radii. These canals are not in the center of the plates but displaced to the peripherie thus delimiting a thinner solid outer lamina and a thicker inner one. The longitudinal canals are open at the junction of the parietes to the basal disk but closed to the top of the shell. The basal edge of the parietes, at the site of the interdigitated junction with the basal disk, looks serrate by the disposition of numerous denticle structures which are separated from each other by the longitudinal canal opening. Along the plates, canals are separated from each other by calcified partitions called septa. The inner side of the plates is smooth, while the outer surface shows numerous undulated ridges running parallel to the base. The ridges superimpose to each other and are formed in relation to each molt.

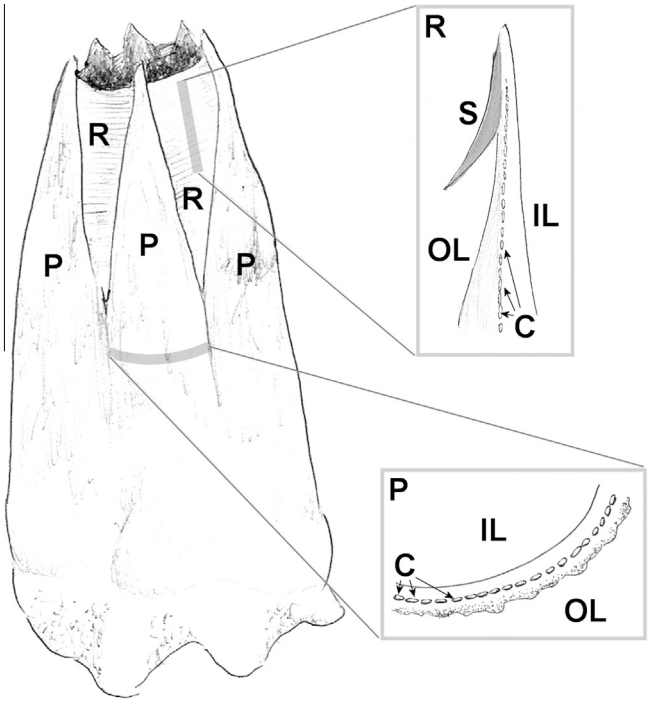

Fig. 1. Schematic illustration of barnacle's shell wall showing parietes (P) and radii (R), longitudinal section of a radius and transversal section of a pariete showing canals (C), outer and inner lamina (OL and IL), and sheath (S).

3.2. Microstructural features

In polished transversal sections of the parietes, it is possible to recognize under the light microscope the presence of numerous parallel light thicker and dark thinner bands within the calcified inner lamina of the shell (Fig. 2a and b). The dark bands are connected to each other by perpendicular even thinner lamellae. The same features are observed around the canals in the form of concentric circular bands. When the same sections are observed under the epifluorescent microscope, the dark bands, viewed under light microcopy, showed autofluorescence (Fig. 2c and d). Although the most internal part of the septa, surrounding the canals, is formed by concentric rings of light and dark bands, the rest of the calcified septa showed a fractal arborescent or tree-like features consisting of a central stalk with numerous perpendicular primary ramifications which once again branches to secondary ones (Fig. 2a). While the top of these tree-like structures faces de inner lamina of the shell, the central stalk forms the center of the septa and projects radially to the outer lamina. In a longitudinal view of the shell, the tree-like structures are projections of the denticles observed in the bottom of the parietes, while the dark lines are in fact the walls of concentric truncated cones forming the inner lamina of the shell or the walls of concentric cylinders forming the canals.

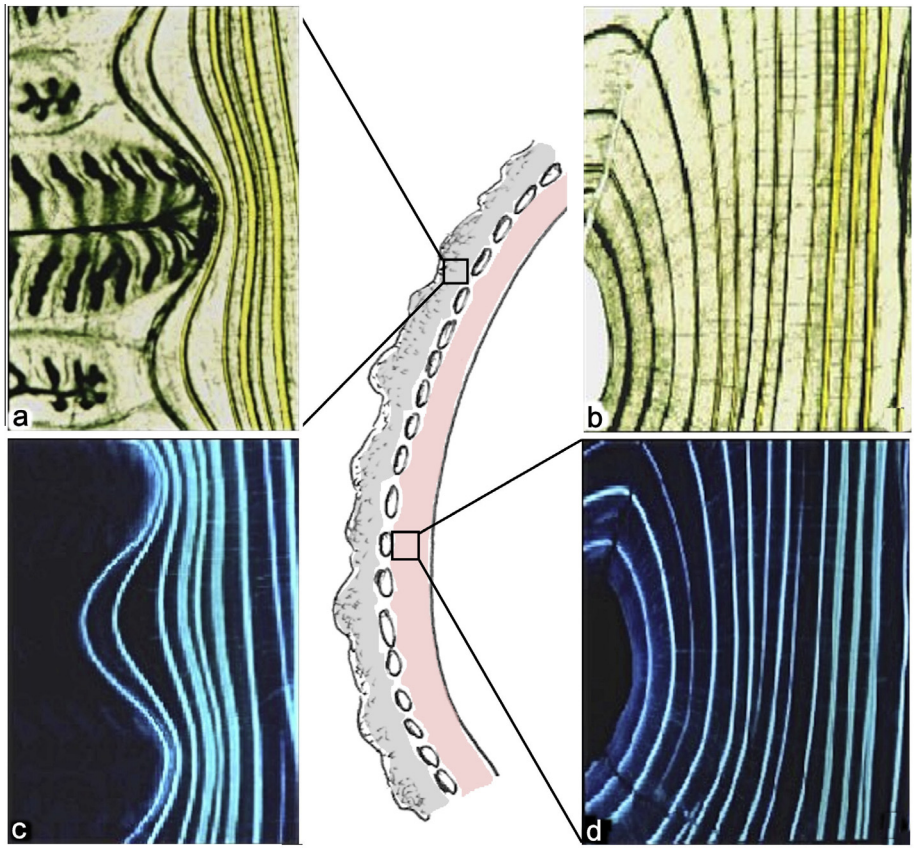

Fig. 2. Light microscopy of polished transversal sections of a paries showing numerous parallel light thicker and dark thinner bands within the calcified outer (a) and inner (b) lamina of the shell. 400×. Same sections observed under the epifluorescent microscope showing autofluorescence of the dark bands forming rings around canals and sheets layering the inner lamina (c) and (d). The calcified septa showed a fractal arborescent or tree-like features consisting of a central stalk with numerous perpendicular primary ramifications which once again branches to secondary ones, and are not autofluorescent (a) and (c). 400×. Schematic illustration of barnaclés paries is in the center of the figure.

3.3. Ultrastructural and chemical features

When the parietes are observed by scanning electron microscopy after sequential decalcification, it was shown that the decalcification-sensitive material was removed from the region corresponding to the light bands observed under the light microscope (Fig. 3a–c) located between two protruding narrow bands which in turn, correspond to the dark thinner bands observed under light microcopy. When decalcified samples were observed by transmission electron microcopy, the dark (light microscopy) protruding (SEM) bands are formed by two dozen of parallel periodic lamellae (Fig. 3d) and mainly correspond to the deproteinized insoluble fraction (DIF). The main component of the DIF is chitin (Fig. 4). A closer look to the FTIR spectrum showed the amide I band splitted into two components at about 1660 and 1630 cm^{-1} corresponding to α chitin (Fig. 4 insert), as has been described for α-chitin of other biological sources (Brunner et al., 2009; Focher et al., 1992; Jang et al., 2004; Kumirska et al., 2010; Pearson et al., 1960). Lamellae showed immunogold positive reaction against anti-keratan sulfate antibody (Fig. 5a), while reticular matrix between bands showed positive reaction to anti-dermatan sulfate and chondroitin-6-sulfate (Fig. 5b and c). All the antibodies used here showed a positive reaction for the SF and PGEF material (Fig. 6). However, reaction was especially intense for DS and KS in the PGEF compared with the SF material, while reaction to C-6-S was similar in both fractions. It is important to remember that quantitative comparisons should only be done between reactivities of different samples to the same antibody because of the difference in the sensitivity of each antibody against its own antigen.

3.4. In vitro crystallization features

When crystallization assays were carried out in the absence of any organic additive, regular calcite crystals showing the {1 0 4} faces were obtained (Fig. 7a–c). When IF from formic acid decalcification was added to the calcium solution, the crystals formed on the bottom of the microbridges do not showed any significant morphological modification compared with the control crystals (Fig. 7d). However, the crystals formed on the insoluble chitin fibrillar material appeared as aggregations of calcite crystals where the corners of the rhombohedral crystals became rough and started to develop curved faces together with rounded vaterite crystals (Fig. 7e). Interestingly, when the same insoluble fraction was used but deproteinized, crystals associated to the chitin fibers maintain their rhombohedral {1 0 4} faces (Fig 7f). On the other hand, when SF was added to the crystallization system, a time-depending modification of the crystals morphology and polymorphism occurrence was observed. The addition of SF for 6 h, formed predominately vaterite crystals (Fig. 7g), while a combination of vaterite and rounded faces calcite is formed at 8 h and, only less curved face calcites are found at 20 h of incubation (Fig. 7h and i). Results of incubation with IF obtained after Dowex decalcification are quite different from those of formic acid decalcification fractions. In fact, IF Dowex fraction produced heavy curved face calcite crystals and big vaterite aggregations (Fig. 8a and b), while non modified calcite crystals are formed on the chitin fibers obtained after deproteinization of Dowex IF (Fig. 8c). When proteoglycan enriched fractions were used, piles of modified calcite crystals grow with their *c*-axis aligned (Fig 8d–f).

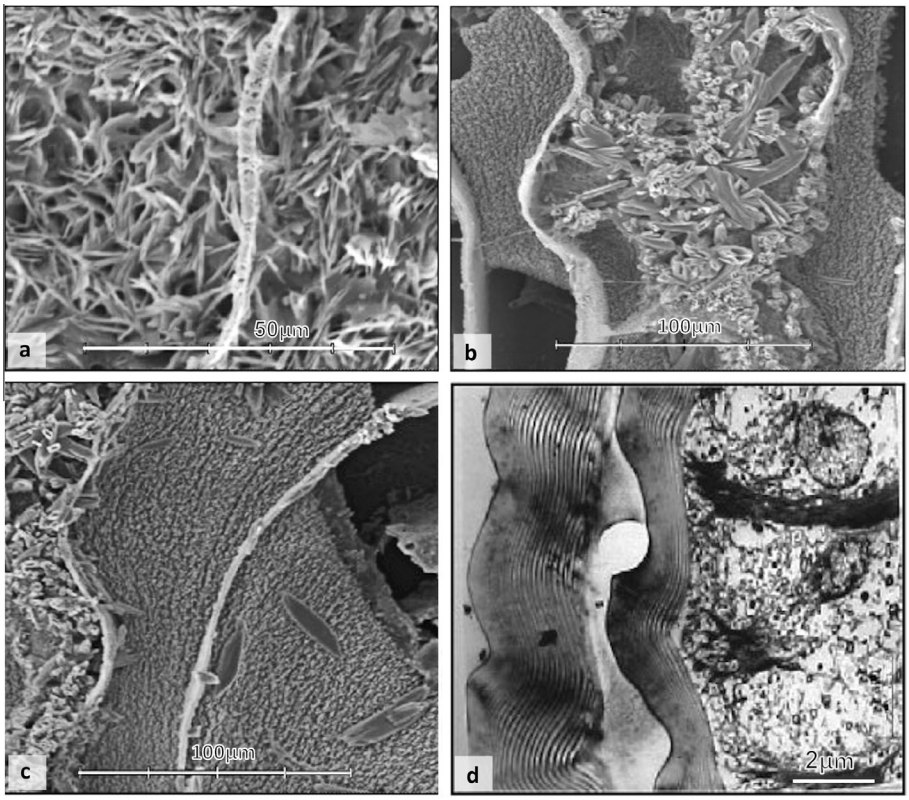

Fig. 3. SEM of partially decalcified shell showing elongated crystals associated to granular organic material between chitin sheets (a) 15 s decalcification, 330×; (b) 30 s decalcification, 670×; (c) 50 s decalcification, 670×. (d) TEM of a decalcified shell on the mineralization front showing mantle cells (right) and laminated sheets of chitin and a granular material between them. 4.400×.

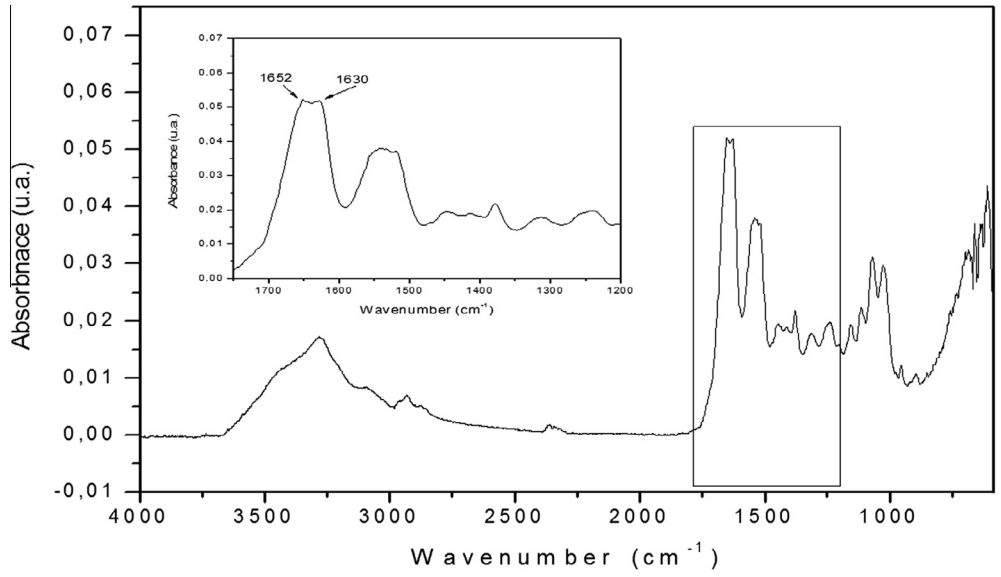

Fig. 4. Fourier transform infrared spectrum of deproteinized insoluble fraction (DIF) showing α-chitin spectrum (insert).

4. Discussion

The most abundant biogenic mineral is calcium carbonate, which exist in different polymorphs: calcite, aragonite, vaterite, and amorphous $CaCO_3$, listed in order of decreasing thermodynamic stability under normal conditions.

As it has been described in other biomineralized structures such as egg- and mollusk-shells (Arias et al., 1993; Mann, 2001; Nys et al., 1999), the organic components in the barnacle shell only represent a small fraction of the total mass. While the inorganic phase in all these models is calcium carbonate, the distribution and composition of the intra- and intercrystalline macromolecules varies considerably, suggesting that they play a decisive role in the nucleation, growth, morphology, texture and polymorphic selection of the inorganic crystalline phase.

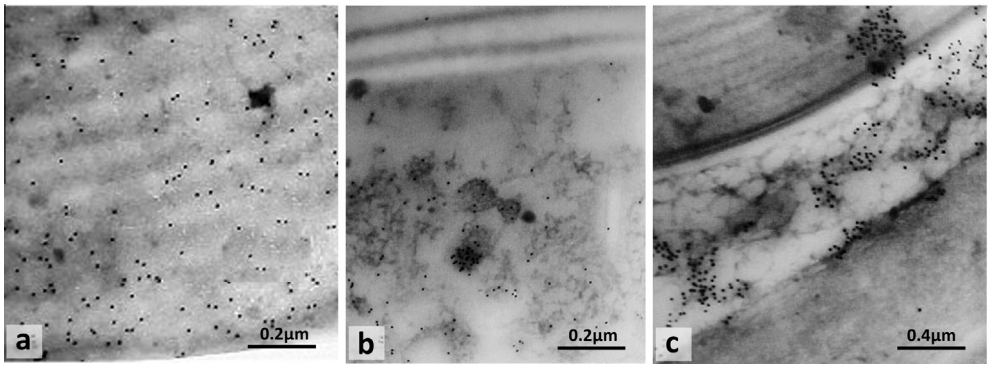

Fig. 5. TEM immunogold reaction of a decalcified shell. Lamellae showed immunogold positive reaction against anti-keratan sulfate antibody (a) 50.000×, while reticular matrix between bands showed positive reaction to anti-dermatan sulfate (b) 30.000× and anti-chondroitin-6-sulfate (c) 80.000.

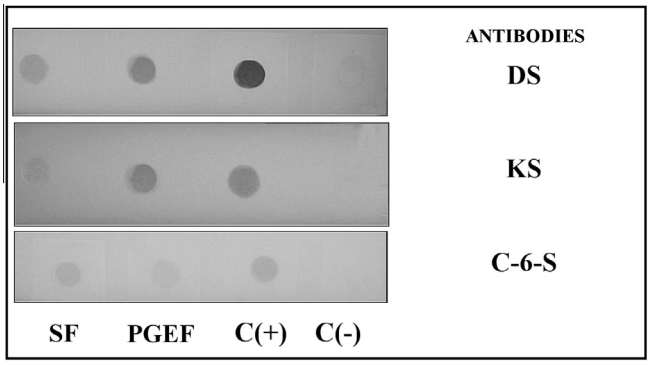

Fig. 6. Dot-blot analysis of material extracted from barnacle shell. SF: shell soluble fraction; PGEF: proteoglycan enriched fraction. DS: dermatan sulfate; KS: keratan sulfate; C-6-S: chondroitin-6-sulfate. Cartilage proteoglycans from bovine nasal septum and from Day 8 chick limb bud chondrocyte cultures were used as positive controls (C+) for antibodies to C-6-S, DS and KS, while proteoglycans from rat chondrosarcoma were used as the negative control for the KS antibodies and omission of primary antibody from the dot-blots for C-6-S, DS (C−).

Here we show that the barnacle shell is organized as a series of mineralized layers, separated by concentric lamellae of organic matrix. The main component of these lamellae is chitin, but in order to obtain an infrared spectrum equivalent to that of standard chitin, it was necessary to treat the lamellae organic matter with NaOH, indicating that chitin is closely associated to proteins. This association is not unique of barnacle shell but occurs also in other crustacean calcified structures (Glazer and Sagi, 2012; Glazer et al., 2010; Ishii et al., 1998; Thormann et al., 2012), and in fact the industrial isolation of chitin, from different sources, requires a deproteination process, often consisting in treatment with NaOH (Khor, 2001). Although such treatments resulted in the partial deacetylation of chitin, forming chitosan, what is evidenced by infrared spectroscopy as an increase of the absorbance in the region of 1.655 cm^{-1} associated to the presence of CO groups (Monteiro and Airoldi, 1999), the treatment conditions used here, did not affected significantly the structure of the chitin obtained, but substantially removed the associated-proteins. Although these chitin-associated proteins have not been characterized yet, it is expected that they contain tryptophan and tyrosine residues, which could be responsible for the considerable autofluorescence observed prior to the deproteination process.

When the insoluble fraction containing chitin was treated with a proteoglycan-extracting solution, a keratan- and dermatan sulfated-rich fraction was obtained. There are few reports on the occurrence of proteoglycans in calcium carbonate-based biominerals or in the shell-forming cells (Dauphin, 2003; Marxen et al., 1998; Marxen and Becker, 2000; Pereira-Mouriès et al., 2002; Poncet et al., 2000). Here we demonstrated the occurrence and precise localization of defined proteoglycans in the barnacle shell. The glycosaminoglycan content of these proteoglycans appeared to share the functionality with those occurred in the avian eggshell (Arias and Fernandez, 2001; Fernandez et al., 2001). In fact, although we cannot discard the simultaneous occurrence of undefined proteins in the barnaclés shell, we do show the occurrence and precise localization of particular proteoglycans. The same proteoglycans have been observed in the avian eggshell where a keratan sulfate-rich proteoglycan (mammalian) has a role in the nucleation of the first calcite crystals, and a dermatan sulfate-rich proteoglycan (ovoglycan) regulates the growth and orientation of the later forming calcite crystals (Arias and Fernandez, 2001; Fernandez et al., 2001).

We have previously showed that the external part of the shell has a massive microstructure consisting of randomly oriented crystals. Toward the interior, the shell became organized in mineral layers separated by thin organic sheets. Each of these mineral layers has a massive microstructure constituted by highly oriented calcite microcrystals with their *c*-axes aligned [(001) fiber texture] perpendicular to the organic sheets and the shell surface (Rodríguez-Navarro et al., 2006). Here we provide additional evidence supporting the fact that the organic matrix is responsible for the organization of the shell mineral and exerts strong influence on the polymorphism, size and orientation of shell-forming crystals.

According to Oswald step rule, crystallization of $CaCO_3$ occurred by a time sequence of polymorphs transformation (Ogino et al., 1987). In fact, different $CaCO_3$ polymorphs (calcite, aragonite and vaterite) can be formed depending on the conditions of crystallization. Calcite is the most thermodynamically stable polymorph, but vaterite and aragonite can form under specific kinetic conditions and be precursors of calcite. Other studies related to $CaCO_3$ nucleation and the influence of proteins on $CaCO_3$ formation, have involved formation of $CaCO_3$ crystals by vapor diffusion with set-ups similar to that used in the present study (Gómez-Morales et al., 2010; Hernández-Hernández et al., 2008). In these studies it was shown that not only the concentration and nature of the additive influence nucleation and the specific polymorph(s) formed, but also the way in which the experimental system becomes supersaturated influences such variables. In fact, Gómez-Morales et al. (2010) have shown that under the conditions of their experimental set-up, calcite, aragonite and vaterite precipitated in the absence of any additive. However, with the same chamber we have demonstrated that, using buffered solutions, it is possible to select only calcite or a mixture of two or three polymorphs, depending on the diameter of the central hole (controlled

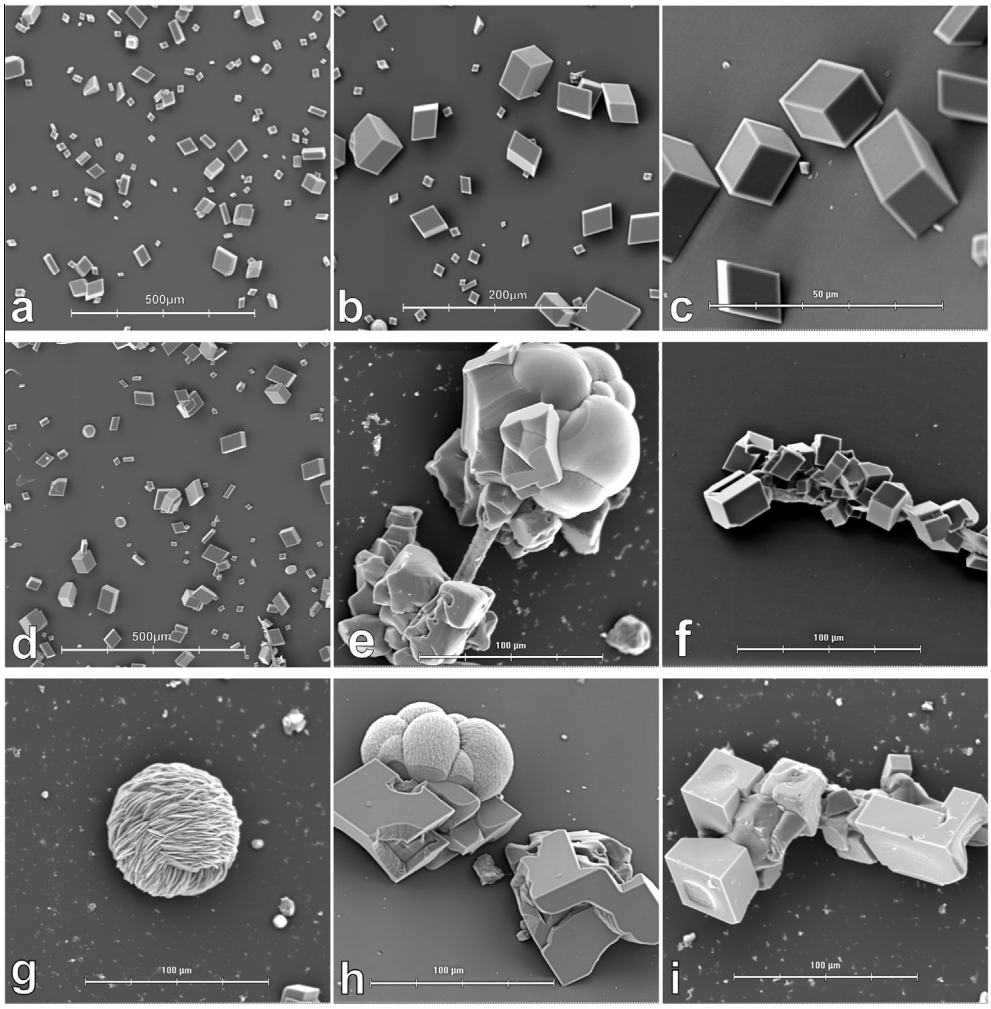

Fig. 7. (a)–(c) Crystallization assays in the absence of any additive showing regular rhombohedral calcite crystals. (d) Crystallization assays in the presence of insoluble fraction from formic acid decalcification showing regular calcite the crystals formed on the bottom of the microbridges. (e) Crystals formed on the insoluble chitin fibrillar material before deproteinized appeared as aggregations of calcite crystals with curved corned and faces. (f). Crystals grown on deproteinized insoluble chitin fibrillar maintain their rhombohedral {1 0 4} faces. (g) Addition of SF for 6 h form predominately vaterite crystals, while a combination of vaterite and calcite is formed at 8 h and, only curved face calcites are found at 20 h of incubation (h) and (i).

gas diffusion) or by altering the time of incubation or the incubation temperature (Neira et al., 2004).

As has been reviewed elsewhere, some additives selectively allow the development of specific crystal faces, while inhibiting others (Gower, 2008; Meldrum and Cölfen, 2008; Sommerdijk and de With, 2008). Ultimately, selective inhibition of calcite growth can favor the formation of less stable forms, vaterite and aragonite.

When different fractions obtained from barnacle shell are added to a system of calcium carbonate growth in vitro, it is possible to observe their effect on the morphology of the crystals formed. That is, when shell soluble fractions, containing mainly proteins and proteoglycans to a lesser extent, were used, is was possible to observe that, depending of the time of incubation, together with vaterite crystals, modified calcite crystals showing new (1 0 1) faces are observed. With incubation time, calcite crystals with stable [1 0 4] faces start to appear while vaterite completely disappeared. A similar effects was found when crystals are grown in the presence of the barnacle shell insoluble fraction containing chitin and proteoglycans. However, when deproteinized chitin fraction is used, rhombohedrical calcite crystals identical to those obtained in the absence of any additive are produced. The same feature is observed when crystals are grown in the presence of proteoglycans enriched fractions where aggregations of rounded calcites are aligned in piles. Albeck et al. (1996) have shown that while the polyanionic nature of some sea urchin proteins allow the expression of crystalline faces other tan [1 0 4], the polysaccharide fraction of these glycoproteins would be involved in the appearance of curvatures in the calcite crystals obtained. However, these authors did not explore the activity of proteoglycans. Such polyanionic macromolecules have been involved in eggshell and crustacean gastrolith structure and formation (Arias and Fernandez, 2008; Arias et al., 2007; Fernández et al., 2012; Luquet et al., 2013).

Our results indicate that, in the barnacle model, proteoglycans are good candidates for the modification of the calcite crystal morphology, although the cooperative effect of some additional proteins in the shell could not be excluded. Up to date, the majority of the studies on the effect of biomacromolecules on biomineralization has been focused on the effect of protein fractions. However, the associated effect of a considerable number and chemical structure of ionic polysaccharide chains occurring in glycoproteins and proteoglycans could increase the diversity of chemical and physical interaction with the calcium carbonate amorphous or crystalline phases.

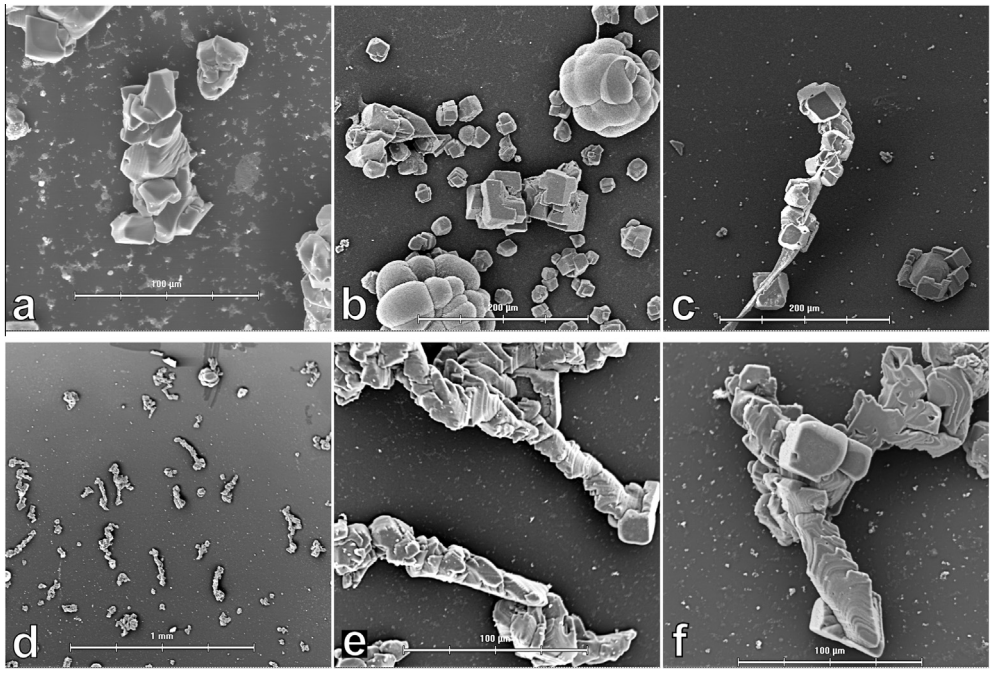

Fig. 8. Crystallization assays in the presence of insoluble fraction from Dowex produced heavy curved face calcite crystals and big vaterite aggregations (a) and (b), while non modified calcite crystals are formed on the chitin fibers obtained after deproteinization of this fraction (c). Crystallization assays in the presence of proteoglycan enriched fractions produce piles of aligned modified calcite crystals (d)–(f).

Acknowledgment

This work was supported by FONDECYT 1120172, granted by the Chilean Council for Science and Technology (CONICYT).

References

Albeck, S., Weiner, S., Addadi, L., 1996. Polysaccharides of intracrystalline glycoproteins modulate calcite crystal growth in vitro. Chem. Eur. J. 2, 278–284.
Arias, J.L., Carrino, D.A., Fernández, M.S., Rodriguez, J.P., Dennis, J.E., Caplan, A.I., 1992. Partial biochemical and immunochemical characterization of avian eggshell extracellular matrices. Arch. Biochem. Biophys. 298, 293–302.
Arias, J.L., Fink, D.J., Xiao, S., Heuer, A.H., Caplan, A.I., 1993. Biomineralization and eggshells: cell-mediated acellular compartments of mineralized extracellular matrix. Int. Rev. Cytol. 145, 217–250.
Arias, J.L., Fernandez, M.S., 2001. Role of extracellular matrix molecules in shell formation and structure. Worlds Poult. Sci. J. 57, 349–357.
Arias, J.L., Mann, K., Nys, Y., García-Ruiz, J.M., Fernandez, M.S., 2007. Eggshell growth and matrix macromolecules. In: Baeuerlein, E. (Ed.), Handbook of Biomineralization, vol. 1. Wiley-VCH, Weinheim, Germany, pp. 309–327.
Arias, J.L., Fernandez, M.S., 2008. Polysaccharides and proteoglycans in calcium carbonate-based biomineralization. Chem. Rev. 108, 4475–4482.
Belcher, A.M., Wu, X.H., Christensen, R.J., Hansma, P.K., Stucky, G.D., Morse, D.E., 1996. Control of crystal phase switching and orientation by soluble mollusc-shell proteins. Nature 381, 56–58.
Belcher, A.M., Gooch, E.E., 2000. Protein components an inorganic structure in shell nacre. In: Baeuerlein, E. (Ed.), Biomineralization: From Biology to Biotechnology and Medical Application. Wiley-VCH, Weinheim, Germany, pp. 221–249.
Bourget, E., 1977. Shell structure of sessile barnacles. Le Natur. Canadien 104, 281–323.
Brunner, E., Ehrlich, H., Schupp, P., Hedrich, R., Hunoldt, S., Kammer, M., Machill, S., Paasch, S., Bazhenov, V.V., Kurek, D.V., Arnold, T., Brockmann, S., Ruhnow, M., Born, R., 2009. Chitin based scaffolds are an integral part of the skeleton of the marine demosponge *Ianthella basta*. J. Struct. Biol. 168, 539–547.
Carrino, D.A., Dennis, J.E., Drushel, R.F., Haynesworth, S.E., Caplan, A.I., 1994. Identity of the core proteins of the large chondroitin sulfate proteoglycans synthesized by skeletal muscle and prechondrogenic mesenchyme. Biochem. J. 298, 51–60.
Caterson, B., Christner, J.E., Baker, J.R., 1983. Identification of a monoclonal antibody that specifically recognizes corneal and skeletal keratan sulfate. J. Biol. Chem. 258, 8848–8854.
Caterson, B., Christner, J.E., Baker, J.R., Couchman, J.R., 1985. Production and characterization of monoclonal antibodies directed against connective tissue proteoglycans. Fed. Proc. 44, 386–393.
Caterson, B., Calabro, T., Hampton, A., 1987. Monoclonal antibodies as probes for elucidating proteoglycan structure and function. In: Wight, F.N., Mecham, R.P. (Eds.), Biology of Proteoglycans. Academic Press, London, pp. 1–28.
Checa, A.G., Rodriguez-Navarro, A., 2001. Geometrical and crystallographic constraints determine the self-organization of shell microstructures in Unionidae (Bivalvia: Mollusca). Proc. R. Soc. B: Biol. Sci. 268, 771–778.
Christner, J.E., Caterson, B., Baker, J.R., 1980. Immunological determinants of proteoglycans. Antibodies against the unsaturated oligosaccharide products of chondroitinase ABC digested cartilage proteoglycans. J. Biol. Chem. 255, 7102–7105.
Darwin, C., 1854. A monograph on the sub-class Cirripedia, with figures of all the species. The Balanidae (or sessile cirripedes; the Verucidae, etc.). Volume II. The Ray Society, London, p. 684.
Dominguez-Vera, J.M., Gautron, J., Garcia-Ruiz, J.M., Nys, Y., 2000. The effect of avian uterine fluid on the growth behavior of calcite crystals. Poult. Sci. 79, 901–907.
Dauphin, Y., 2001. Comparative studies of skeletal soluble matrices from some Scleractinian corals and Molluscs. Int. J. Biol. Macromol. 28, 293–304.
Falini, G., Albeck, S., Weiner, S., Addadi, L., 1996. Control of aragonite or calcite polymorphism by mollusk shell macromolecules. Science 271, 67–69.
Fernandez, M.S., Araya, M., Arias, J.L., 1997. Eggshells are shaped by a precise spatio-temporal arrangement of sequentially deposited macromolecules. Matrix Biol. 16, 13–20.
Fernandez, M.S., Moya, A., Lopez, L., Arias, J.L., 2001. Secretion pattern, ultrastructural localization and function of extracellular matrix molecules involved in eggshell formation. Matrix Biol. 19, 793–803.
Fernandez, M.S., Vergara, I., Oyarzun, A., Arias, J.I., Rodriguez, R., Wiff, J.P., Fuenzalida, V., Arias, J.L., 2002. Extracellular matrix molecules involved in barnacle's shell mineralization. In: J. Aizenberg, J. McKittrick, C. Orme, (Eds.), Biological and Biomimetic Materials – Properties to Function, Mat. Res. Soc. Symp. Proc., Warrendale, PA, 724, 3-9.
Fernández, M.S., Bustos, C., Luquet, G., Saez, D., Neira-Carrillo, A., Corneillat, M., Alcaraz, G., Arias, J.L., 2012. Proteoglycan occurrence in gastrolith of the crayfish *Cherax quadricarinatus* (Crustacea, Malacostraca, Decapoda). J. Crustacean Biol. 32, 802–815.
Focher, B., Naggi, A., Torri, G., Cosani, A., Terbojevich, M., 1992. Structural differences between chitin polymorphs and their precipitates from solutions-evidence from CP-MAS 13CNMR, FT-IR and FT-Raman spectroscopy. Carbohydr. Polym. 17, 97–102.
Glazer, L., Shechter, A., Tom, M., Yudkovski, Y., Weil, S., Aflalo, E.D., Pamuru, R.R., Khalaila, I., Bentov, S., Berman, A., Sagi, A.J., 2010. A protein involved in the assembly of an extracellular calcium storage matrix. Biol. Chem. 285, 12831–12839.
Glazer, L., Sagi, A., 2012. On the involvement of proteins in the assembly of the crayfish gastrolith extracellular matrix. Invertebr. Reprod. Dev. 56, 57–65.
Gómez-Morales, J., Hernández-Hernández, A., Sazaki, G., García-Ruiz, J.M., 2010. Nucleation and polymorphism of calcium carbonate by a vapor diffusion sitting drop crystallization technique. Cryst. Growth Des. 10, 963–969.

Gower, L.B., 2008. Biomimetic model systems for investigating the amorphous precursor pathway and its role in biomineralization. Chem. Rev. 108, 4551–4627.
Hernández-Hernández, A., Rodríguez-Navarro, A.B., Gómez-Morales, J., Jiménez-Lopez, C., Nys, Y., García-Ruiz, J.M., 2008. Influence of model globular proteins with different isoelectric points on the precipitation of calcium carbonate. Cryst. Growth Des. 8, 1495–1502.
Heuer, A.H., Fink, D.J., Laraia, V.J., Arias, J.L., Calvert, P.D., Kendall, K., Messing, G.L., Rieke, P.C., Thompson, D.H., Wheeler, A.P., Veis, A., Caplan, A.I., 1992. Innovative materials processing strategies: a biomimetic approach. Science 255, 1098–1105.
Ishii, K., Tsutsui, N., Watanabe, T., Yanagisawa, T., Nagasawa, H., 1998. Solubilization and chemical characterization of an insoluble matrix protein in the gastroliths of a crayfish, *Procambarus clarkii*. Biosci. Biotechnol. Biochem. 62, 291–296.
Jang, M.K., Kong, B.G., Jeong, X.I., Lee, C.H., Nah, J.W., 2004. Physicochemical characterization of α-chitin, β-chitin, and γ-chitin separated from natural sources. J. Polym. Sci. A 42, 3423–3432.
Jiménez-Lopez, C., Rodriguez-Navarro, A., Domínguez-Vera, J.M., García-Ruiz, J.M., 2003. Influence of lysozyme on the precipitation of calcium carbonate: a kinetic and morphologic study. Geochim. Cosmochim. Acta 67, 1667–1676.
Kamat, S., Su, X., Ballarini, R., Heuer, A.H., 2000. Structural basis for the fracture toughness of the shell of the conch *Strombus gigas*. Nature 405, 1036–1040.
Kamino, K., Inoue, K., Maruyama, T., Takamatsu, N., Harayama, S., Shizuri, Y., 2000. Barnacle cement proteins: importance of disulfide bonds in their insolubility. J. Biol. Chem. 275, 27360–27365.
Khor, E., 2001. Chitin: Fulfilling a Biomaterials Promise. Elsevier Science & Technol, N.Y., 136 pp.
Kumirska, J., Czerwicka, M., Kaczyúski, Z., Bychowska, A., Brzozowski, K., Thöming, J., Stepnowski, P., 2010. Application of spectroscopic methods for structural analysis of chitin and chitosan. Mar. Drugs 8, 1567–1636.
Lennon, D.P., Carrino, D.A., Baber, M.A., Caplan, A.I., 1991. Generation of a monoclonal-antibody against avian small dermatan sulfate proteoglycan: immunolocalization and tissue distribution of PG-II (decorin) in embryonic-tissues. Matrix 11, 412–427.
Lowenstam, H.A., Weiner, S., 1989. On Biomineralization. Oxford University Press, Oxford, p. 324.
Lowenstam, H.A., Weiner, S., Newman, W.A., 1992. Carbonate apatite-containing shell plates of a barnacle (Cirripedia). In: Slavkin, H., Price, P. (Eds.), Chemistry and Biology of Mineralized Tissues. Excerpta Medica, Amsterdam, pp. 73–84.
Luquet, G., Fernández, M.S., Badou, A., Guichard, N., Le Roy, N., Corneillat, M., Alcaraz, G., Arias, J.L., 2013. Comparative ultrastructure and carbohydrate composition of gastroliths from Astacidae, Parastacidae and Cambaridae freshwater crayfish (Crustacea, Decapoda). Biomolecules 3, 18–38.
Mann, S., Webb, J., Williams, R.J.P., 1989. Biomineralization. VCH, Weinheim, Germany, p. 490.
Mann, S., 2001. Biomineralization. Oxford University Press, Oxford, UK, p. 198.
Marxen, J.L., Becker, W., 2000. Calcium binding constituents of the organic shell matrix from the freshwater snail *Biomphalaria glabrata*. Comp. Biochem. Physiol. B 127, 235–242.
Marxen, J.L., Hammer, M., Gehrke, T., Becker, W., 1998. Carbohydrates of the organic shell matrix and the shell-forming tissue of the snail *Biomphalaria glabrata* (Say). Biol. Bull. 194, 231–240.
Mehmet, H., Scudder, P., Tang, P.W., Hounsell, E.F., Caterson, B., Feizi, T., 1986. The antigenic determinants recognized by three monoclonal antibodies to keratan sulfate involve sulfate hepta- or larger oligosaccharides of the Poly(N-acetyllactosamine) series. Eur. J. Biochem. 15, 385–391.
Meldrum, F.C., Cölfen, H., 2008. Controlling mineral morphologies and structures in biological and synthetic systems. Chem. Rev. 108, 4332–4432.
Monteiro, O.A.C., Airoldi, C., 1999. Some thermodynamic data on copper-chitin and copper-chitosan biopolymer interactions. J. Colloid Interface Sci. 212, 212–219.
Neira, A.C., Fernandez, M.S., Retuert, J., Arias, J.L., 2004. Effect of the crystallization chamber design on the polymorphs of calcium carbonate using the sitting-drop method. In: Barron, A.E., Klok, H-A., Deming, T.J. (Eds.). Architecture and Application of Biomaterials and Biomolecular Materials, Mat. Res. Soc. Symp. Proc. EXS-1:321-326.
No, H.K., Meyers, S.P., 1997. Preparation of chitin and chitosan. In: Muzzarelli, R.A. A., Peter, M.G. (Eds.), Chitin Handbook. European Chitin Society, pp. 475–489.
Nys, Y., Hincke, M., Arias, J.L., García-Ruiz, J.M., Solomon, S., 1999. Avian eggshell mineralization. Poult. Avian Biol. Rev. 10, 142–166.
Ogino, T., Suzuki, T., Sawada, K., 1987. The formation and transformation mechanism of calcium carbonate in water. Geochim. Cosmochim. Acta 51, 2757–2767.
Orme, C.A., Noy, A., Wierzbicki, A., McBride, M.T., Grantham, M., Teng, H.H., Dove, P. M., DeYoreo, J.J., 2001. Formation of chiral morphologies through selective binding of amino acids to calcite surface steps. Nature 411, 775–779.
Pearson, F.G., Marchessault, R.H., Liang, C.Y., 1960. Infrared spectra of crystalline polysaccharides. V. Chitin. J. Polym. Sci. 13, 101–116.
Percot, A., Viton, C., Domard, A., 2003. Characterization of shrimp shell deproteinization. Biomacromolecules 4, 1380–1385.
Pereira-Mouriès, L., Almeida, M.J., Ribeiro, C., Pedizzi, J., Barthélemy, M., Milet, C., Lopez, E., 2002. Soluble silk-like organic matrix in the nacreous layer of the bivalve *Pinctada maxima*. Eur. J. Biochem. 269, 4994–5003.
Poncet, J.M., Serpentini, A., Thiébot, B., Villers, C., Bocquet, J., Boucaud-Camou, E., Lebel, J.M., 2000. In vitro synthesis of proteoglycans and collagen in primary cultures of mantle cells from the nacreous mollusk, *Haliotis tuberculata*: a new model for study of molluscan extracellular matrix. Mar. Biotechnol. 2, 387–398.
Rodríguez-Navarro, A., Cabral de Melo, C., Batista, N., Morimoto, N., Alvarez-Lloret, P., Ortega-Huertas, M., Fuenzalida, V.M., Arias, J.I., Wiff, J.P., Arias, J.L., 2006. Microstructure and crystallographic-texture of giant barnacle (*Austromegabalanus psittacus*) shell. J. Struct. Biol. 156, 355–362.
Simkiss, K., Wilbur, K.M., 1989. Biomineralization. Academic Press, San Diego, p. 337.
Smith, B.L., Schäffer, T., Viani, M., Thompson, J.B., Frederick, N.A., Kindt, J., Belcher, A. M., Stucky, G.D., Morse, D.E., Hansma, P.K., 1999. Molecular mechanistic origin of the toughness of natural adhesives, fibres and composites. Nature 399, 761–763.
Sommerdijk, N.A.J.M., de With, G., 2008. Biomimetic $CaCO_3$ mineralization using designer molecules and interfaces. Chem. Rev. 108, 4499–4550.
Su, X.W., Belcher, A.M., Zaremba, C.M., Morse, D.E., Stucky, G.D., Heuer, A.H., 2002. Structural and microstructural characterization of the growth lines and prismatic microarchitecture in red abalone shell and the microstructures of abalone "flat pearls". Chem. Mater. 14, 3106–3117.
Thormann, E., Mizuno, H., Jansson, K., Hedim, N., Fernández, M.S., Arias, J.L., Rutland, M.W., Pai, R.K., Bergström, L., 2012. Embedded proteins and sacrificial bonds provide the strong adhesive properties of gastroliths. Nanoscale 4, 3910–3916.
Yanagishita, M., Hascall, V.C., 1984. Proteoglycans synthesized by rat ovarian granulosa cells in culture. Isolation, fractionation, and characterization of proteoglycans associated with the cell layer. J. Biol. Chem. 259, 10260–10269.